NANO LETTERS

2005
Vol. 5, No. 7
1255−1260

Hierarchical Self-Assembly of a Coiled-Coil Peptide into Fractal Structure

Andrea Lomander,[†] Wonmuk Hwang,[†] and Shuguang Zhang*[,†,‡]

Center for Biomedical Engineering, and Center for Bits & Atoms, Massachusetts Institute of Technology, Cambridge, Massachusetts 02139-4307

Received February 1, 2005

ABSTRACT

Here we report the hierarchical self-assembly of a cross-linkable coiled-coil peptide containing an internal cysteine. Atomic force microscopy (AFM) experiments revealed the fractal structure of the assemblies, and molecular simulations showed that the peptides cross-linked to form clusters of coiled-coils, which further assembled to form globules of tens of nanometers in diameter. Such hierarchical organization was modulated by pH or thiol-reducing agent. Exploitation of the fractal structures through chemical methods may be valuable for the fabrication of materials spanning multiple length scales.

There is a growing interest and continuous demand in the fabrication of smaller and smaller materials, parts, and features for nanotechnology and nanobiotechnology. One of the most difficult tasks is to produce materials that incorporate multiple length scales simultaneously, from nano and micro, to macro scales. Fractals achieve this goal because of their self-similarity, as demonstrated not only mathematically[1,2] but also in the real world; their uses in biology, chemistry, physics, and engineering are exemplified by numerous observations and computer simulations.[3−10] Therefore, fabrication of fractal structures can be an alternative way to fabricate advanced materials for a broad range of applications.

Fabrication of fractal nanomaterials requires self-assembly since direct manipulation of such self-similar structures at the lower end of the scale is extremely difficult to achieve. Self-assembly of biomolecules has recently emerged as an alternative fabrication method for a variety of material processing, from a few nanometers to a macroscopic scale.[11,12] An emerging field of molecular self-assembly of biological materials can be combined with traditional material processing, melting/solidification, solution processes, and vacuum deposition, so that novel materials can be designed and fabricated. Molecular self-assembly takes place via a subtle balance between noncovalent interactions such as electrostatic and hydrophobic interactions that result in the formation of well-defined structures.[11−16]

We have previously reported the discovery and design of several classes of self-assembling peptides to produce various nanostructures.[12] One example is the formation of a left-handed helical ribbon of uniform geometry through the self-assembly of a β-sheet forming peptide.[17] Another example is the self-assembly of peptide surfactants into nanotubes and nanovesicles.[18−20] Others have used peptide self-assembly to form scaffolds on which various nanostructured organic or inorganic materials are produced.[13−15] One of the key challenges in the fabrication of new materials via such bottom-up technology is the organization of nanostructures across a wide spectrum of length scales.[11−16]

Here we report the formation of fractal structures from a self-assembling coiled-coil peptide. We introduced a cysteine at the N-terminus of the peptide sequence and studied its self-assembly behaviors. The self-assembly of the coiled-coils occurred in two different ways: one of which was through the well-known noncovalent intertwining on one side of the peptides, and the other one was through the cysteine disulfide bond that covalently linked two peptides that belonged to separate coiled-coils. Cross-linked peptides subsequently formed globules of tens of nanometers in diameter, which further aggregated to form larger clusters up to a few micrometers. When deposited onto a two-dimensional substrate, the globules underwent diffusion-limited aggregation (DLA) to form fractal features. In this process, it is possible to control the structures at several levels, from the primary sequence, the secondary and tertiary structures of individual molecules, to the mesoscopic morphology of the fractals formed on the substrate, by adjusting the solution conditions. Optimization and further modifica-

* Corresponding author. Shuguang Zhang, Center for Biomedical Engineering NE47−379, Massachusetts Institute of Technology, Cambridge, MA 02139-4307. E-mail: shuguang@mit.edu. Tel: 617-258-7514. Fax: 617-258-5239.

[†] Center for Biomedical Engineering.

[‡] Center for Bits & Atoms.

10.1021/nl050203r CCC: $30.25
Published on Web 06/07/2005

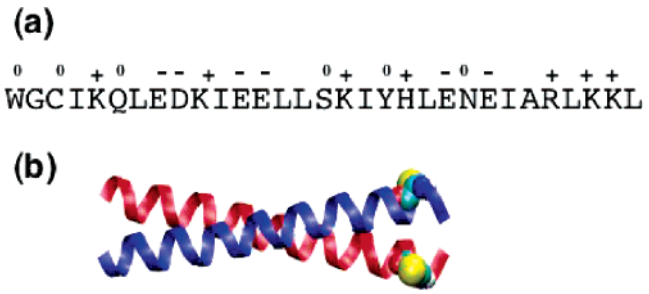

Figure 1. Primary sequence and secondary structure of the coiled-coil peptide. (a) Amino acid sequence of the 31 residue peptide. Charged amino acids are labeled with (+) or (−) and polar amino acids are labeled with (0). (b) Model of a coiled-coil. Note the location and the direction of the cysteines (van der Waals representation). This arrangement limits the size of the cross-linked clusters. Hydrophobic side chains are located between the two α-helices.

tions lead to the use of this peptide system as an environmentally responsive template for fabricating materials.

The 31-residue peptide used in this study was derived from a typical heptad sequence of a coiled-coil,[21,22] in particular, the yeast transcription factor GCN4 (Figure 1). The N- and C-termini of the peptide were acetylated and amidated, respectively, to abolish the intrinsic changes.

We deposited the peptide solution on a freshly cleaved mica surface and examined it by using AFM. The AFM images showed characteristic fractal-like patterns (Figure 2).[1,2] This feature was further confirmed by systematically measuring its fractal dimension, typically defined by the divider formula[23]

$$D_f = \lim_{r \to 0} \frac{\log N(r)}{\log(r)}$$

where r is the length unit, $N(r)$ is the size of the geometric object measured with the unit r. To measure D_f,[24,25] we used a method illustrated in Figure 2a,b on two different divider or ruler scales. Here, N is the contour length measured with the ruler of size r. For a given value of r, the ruler usually cannot walk along the contour exactly with an integer number of steps, giving rise to the mismatch between the start and the endpoints, (points A and B in Figure 2). In such cases, N was calculated as the sum of the number of full steps and the fractional length between the start and the end-points with respect to r. In the example shown in Figure 2a, r = 0.9 μm. It took 28 steps (green lines) starting from point A to proceed to point B along the contour. The remaining distance between A and B (red line) is 0.64 μm, whose fractional length with respect to r is 0.64/0.9 = 0.576. Therefore, the total contour length is 28.576. For r =1.8 μm, the total contour length yielded an average value of N = 10.38 (Figure 2b). The measured value of N depended on the location of the starting point of the contour. Inspired by the Nyquist sampling theorem,[26] several values of N starting at different points on the contour were measured and averaged. The graph of log[r] vs. log[N] gave a straight line, where the absolute value of the slope gave the fractal dimension D_f (Figure 2c).

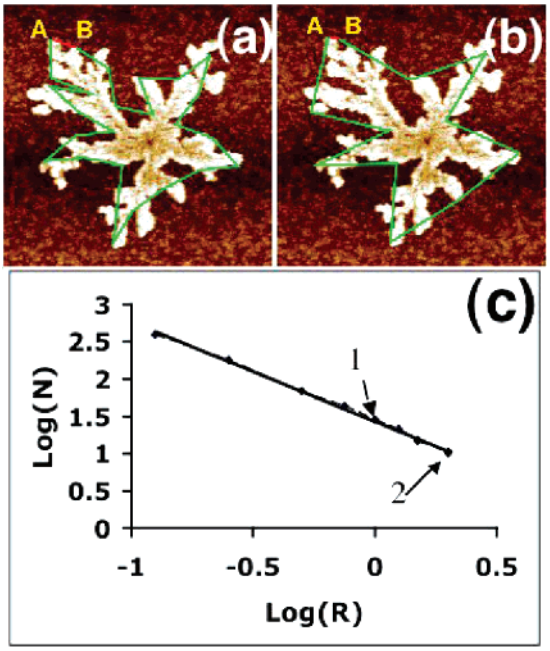

Figure 2. Analysis of the fractal patterns. (a) A straight ruler of length r (green), walks along the nanomaterial surface contour, starting from point A, and ends at point B. Left: r = 0.9 μm, and right: r = 1.8 μm. The distance between A and B (red) is measured to be d. The path length N is then defined as the sum of the number of steps and d/r. (**b**) A log−log graph of N versus r (μm). Arrows: Data points from (a). The fractal dimension, D_f, is the absolute value of the slope, in this case $D_f = |-1.34| = 1.34$.

Since the coiled-coil peptide contained many charged residues (Figure 1a), we studied the effect of pH on the structure formation. The secondary structure of the peptide in all pH ranges showed a typical α-helix with circular dichroism minima at 208 and 221 nm,[27] although the helical content varied with pH[28] (CD profile, see Supporting Information). These findings suggested that the neutralization of the charged side chains did not completely disrupt the secondary structure of the coiled coil. This was possible because the coiled-coil formation was primarily through hydrophobic interaction between the two helices.[17,18] Although protonation of charged residues may weaken the ionic bonds, the basic α-helical coiled-coil structure should remain. On the other hand, addition of acetonitrile (100 mM) or a denaturing agent, guanidine hydrochloride (6 M) eliminated the helical structure (data not shown).

Fractal patterns were found for pH ∼2 when observed under AFM on mica surfaces (Figure 3 a−d). On the other hand, only round or irregular aggregates were observed for pH above 3 (Figure 3e,f). When silicon substrate was used, fractal patterns were observed for pH values both at 1 and 8.5 (images not shown). This can be explained by the fact that the fractal was formed by surface diffusion (see below), and surface diffusion was independent of the solution's pH on the neutral silicon surface, in contrast to a negatively charged mica surface, which is neutral only at very low pH.

Upon closer inspection, it was revealed that the structures consisted of small globules (Figure 3c) that were also present at higher pH. They exhibited a flat, disk topology under AFM, and their dimensions depended on pH: as the pH

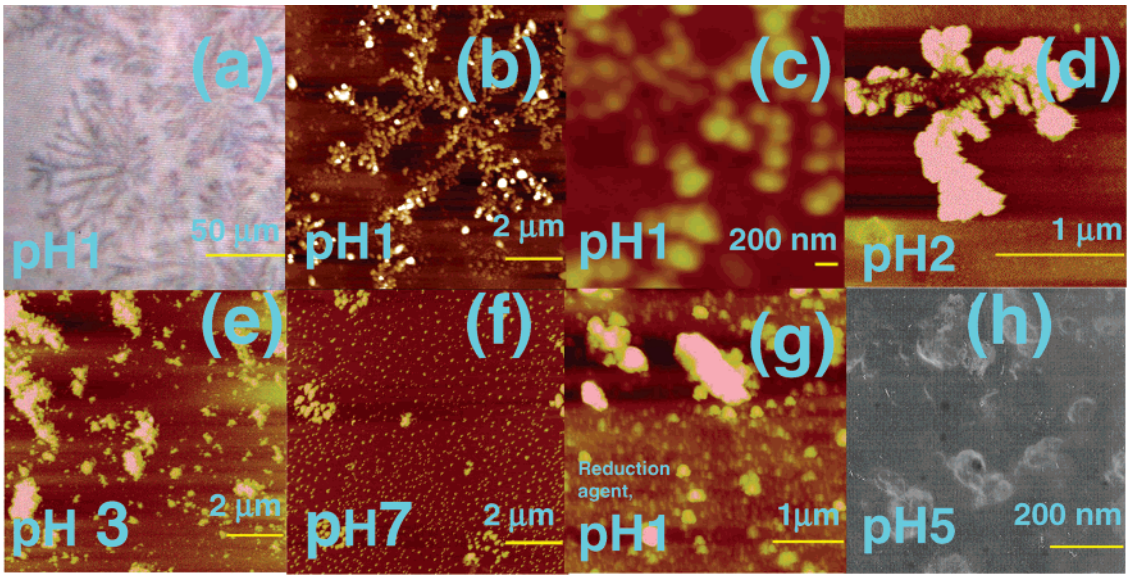

Figure 3. Morphology of coiled-coil assemblies at different pH. (a) Large fractal patterns formed by the peptide at pH 1. Parts of the image were captured on the video monitor used in connection with the AFM. Such patterns were always visible when fractal patterns on the micrometer scale could be imaged (pH 1 and 2). Panels b−g are AFM images. (b) pH 1. (c) Sized up image from (b), pH 1. (d) pH 2. (e) pH 3. (f) pH 7. (g) pH 1, with a reduction agent. (h) Quick-freeze deep-etch transmission electron microscopy image of the peptide at pH 5. Due to low contrast, numerous small globules of diameter 10−20 nm were only visible directly on the film.

increased from 1 to 7 or 8, the disk tended to become thicker (taller and smaller diameter), and became thinner and wider again at pH 9. The reason for this behavior is probably related to the electrostatic screening effect, as discussed in more detail below.

For the peptide samples at pH values less than 3, graphs of log(N) versus log(r) yielded a straight line with an R^2 value between 0.98 and 0.99. Analyses of the slopes of 10 samples provided the magnitude of the slope. This value corresponded to the fractal dimension D_f of a viscous fingering system,[25] whose formation mechanism is known as diffusion-limited aggregation (DLA).[29,30] In the plane, $D_f = 1.71$; however, in real systems, depletion effects may decrease D_f from this ideal value to 1.4.[25−26] We therefore suggest that the fractal feature was formed on the two-dimensional substrate through a DLA-like process.

To further probe aggregation behavior of the coiled-coil peptides in solution, dynamic light scattering (DLS) was performed. The results showed that the size of the clusters was independent of pH (Supporting Information). Using quick-freeze deep-etch transmission electron microscopy, we found a mixture of globules with a diameter ∼20 nm, and larger heterogeneous clusters, reaching up to hundreds of nanometers in diameter (Figure 3h). However, DLS detected only the larger clusters. In the AFM images, large globular regions of similar sizes were also found in the same sample where the structures containing smaller globules were observed.

Since individual pairs of coiled-coil peptides have a radius of gyration of ∼1.4 nm, one globule should be a cluster of many such pairs. The cysteine disulfide bond should remain stable at low pH.[31,32] However, reducing agents, such as β-mercaptoethanol (100 mM) or DTT (420 μM) cleaved the disulfide bond, destroying the clusters into individual coiled-coils. We tested this using polyacrylamide gel electrophoresis (PAGE) under both native and reducing conditions (Figure 4a). In the presence of reducing agents, the cysteine disulfide bonds were disrupted, thus the peptides moved fast (Figure 4a). On the other hand, without the reducing agent, the peptides formed very large clusters that moved very slowly in the gel. Furthermore, addition of a reducing agent also affected the morphology and abolished fractal formation (Figure 3g) below pH 3. Therefore, both the presence of disulfide bonds and maintenance of the coiled-coil structure were likely to be important in the formation of the fractal patterns.

We carried out molecular dynamics (MD) simulations to further study the assembly at the molecular level. The α-helices in coiled-coils are generally known to be arranged in parallel. This packing sterically limits the size of a single cluster. The MD simulation suggested that up to six cross-linked coiled-coils were stable (Figure 4b, left), whereas in seven cross-linked coiled-coils, one of the α-helices could not fit and began to unfold near the cross-linked region (Figure 4b, right). The radius of gyration, R_g, of a coiled-coil was calculated to be 1.4 nm, while the R_g of a hexamer was 3.21 nm. As the globule deposited on the mica surface deformed into a discoid, with the diameter approximately 60 nm and the height 1.7 nm, one can estimate the approximate number of coiled-coils in a globule as 210 (a globule consisting of hexamers only) to 420 (a globule consisting of individual coiled-coils only). It is likely that the globule contains a mixture of clusters, so the number of coiled-coils will vary between these numbers.

Based on our observations, we propose a schematic model to illustrate the self-assembly of our peptide system (Figure 5). Here, two individual peptides formed a coiled-coil to shield their hydrophobic sides. Through the formation of disulfide bonds, up to six coiled-coils could cross-link to

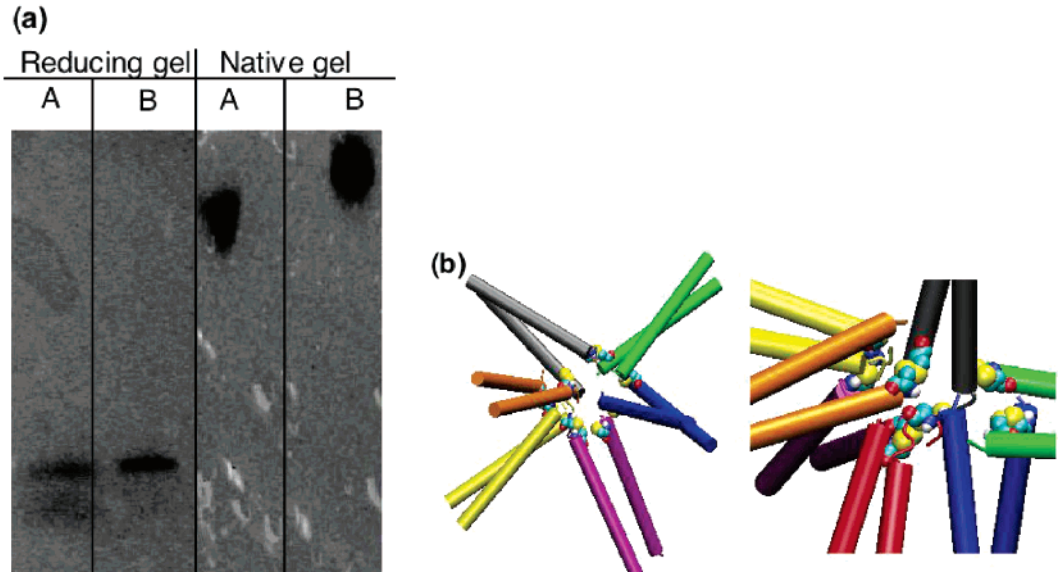

Figure 4. Gel electrophoretic analysis of coiled-coils clusters. (a) PAGE under denaturing (reducing) (sodium dodecyl sulfate, SDS), and native conditions. A = reducing agent (β-mercaptoethanol) in the loading buffer, B = no reducing agent in the loading buffer. Under denaturing conditions, the coiled-coils break into individual peptides, so the solution mostly contains two peptides cross-linked by the disulfide bond. With the reducing agent, the disulfide bond breaks, producing isolated peptides, hence two bands. Under native conditions, the peptide is not denatured in the gel, hence there is a distribution of clusters (broader band). Reducing agent breaks down part of these clusters, shifting the band downward. (b) Molecular dynamics simulations. Left panel: hexamer of the peptide coiled-coils. Right panel: close-up of an unstable heptamer with one of the helices (red) unwinding.

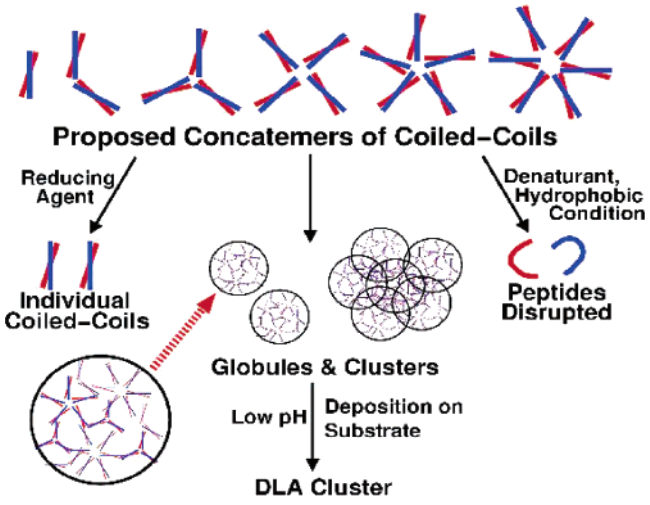

Figure 5. Proposed model of the coiled-coil fractal structural self-assembly process. Coiled-coils could cross-link into clusters, up to hexamers. In solution, they further assemble to form globules and clusters consisting of more than hundreds of coiled-coils. When deposited on a substrate, the globules form DLA clusters. Addition of a reducing agent, denaturant, or a hydrophobic solvent modifies this process. This plausible model explains our observations. The models are not to scale.

form a cluster. These clusters further assembled to form a globule. The size of the globule was presumably determined by the balance between the decrease in entropy and the lowering of the interfacial energy between clusters upon assembly. As the cluster appeared to form a fractal pattern, the contact area between them is small compared to their volume, so that a globule would consist of a loosely connected network through noncovalent interactions, such as ionic and van der Waals interactions.

The high aspect ratio between horizontal and vertical dimensions of the fractals in the AFM image reflected its deformability. Due to loose connectivity, the desolvation penalty upon aggregation is expected to be small, so most of the entropic contribution to the free energy would come from the peptide, rather than the solvent. Thus, larger globules would not be favored, as the entropy would decrease upon aggregation. On the other hand, aggregation lowers the interfacial energy through the formation of noncovalent bonds. The balance between these competing contributions will determine the size of the globule. Once the globules were formed, they behaved as unit colloidal particles and further aggregated into a larger aggregate, whose size grew at higher concentration, as observed through dynamic light scattering. However, whether clusters maintained the identity in the globules, or whether the globules had the same type of loose connectivity is not well understood. Additional systematic experiments and molecular simulations may clarify this.

When the peptide solution was deposited on a surface, all globules in the bulk were confined into two dimensions. This increased the surface concentration of globules that could nucleate a small aggregate. Under favorable conditions, other globules could diffuse on the substrate to form a diffusion limited aggregation cluster from this “seed”. In the case of the mica surface, the solution had to be low in pH in order to neutralize the substrate, since mica could inhibit surface diffusion through the formation of an ionic interaction with positively charged side chains. Such screening effect can also be responsible for the pH dependent change of the disk shape in the AFM images.

At low pH, the peptides were positively charged, so that clusters in the globule were more loosely bound. This resulted in the globule spreading more when deposited on

the substrate (thinner and wider disks). On the other hand, at neutral pH, clusters were more tightly bound, resulting in the globule spreading less (thicker and narrower patterns).

These processes could be perturbed by the addition of a hydrophobic solvent or a denaturing agent. Under such conditions, the basic coiled-coil unit could be disrupted, thus the α-helical structure would not be maintained. Without a stable secondary structure, the aggregation is uncontrolled and only amorphous aggregates were produced, as observed under AFM. Another perturbation could be achieved through the addition of a thiol-reducing agent to produce individual coiled-coils. The geometry of a single coiled-coil allowed clusters to be more compact so that the selection mechanism for the size of the globule would become different through water desolvation. This gave rise to a more heterogeneous distribution of the aggregate sizes (Figure 3g).

Coiled-coil peptide systems have shown to be useful as scaffold for constructing nanostructures. For instance, Zhou, et al.[33] attached four leucine zipper peptides to one nanogold and used it as a building block for fabrication of monodisperse helical fibers. Ryadnov, et al.[34] used "bottom-up" technology for building new structures; one peptide can be used as a template for the assembly of other peptides, as a "belt and braces" system, to link small nanocrystals, such as gold nanoclusters, into a regularly spaced network. Similarly, other metal and semiconductor nanoclusters may be attached to the coiled-coil peptide to build a nanowire for potential control through radio frequency-magnetic field.[35]

Using the designed coiled-coil peptides and other molecular materials to build nanomaterials, for which the self-assembly process can be controlled by common biochemical methods, is a novel approach to achieve multiple length scales simultaneously. It is hoped that our work reported here may stimulate additional research to produce new materials. Using such fractal systems to fabricate nanostructures will likely be a powerful tool for constructing novel materials for a variety of applications.

Materials and Methods. *The Coiled-Coil Peptide.* The 31-residue coiled-coil peptide was commercially synthesized (SynPep, Dublin, CA, www.synpep.com) and dissolved in deionized water, then filtered though a 0.2 μm filter. The solution concentration was adjusted to 230 μM and stored at −20 °C until further use.

Circular Dichrosim. For CD measurements, we used an Aviv 215 CD spectrometer (Aviv Instruments, Lakewood, NJ). We measured a 5 μM sample under various pH conditions. A 5 mm path-length quartz cuvette was used, and signals in milli-degree were converted to molar residue ellipticity. The protocol for the atomic force microscopy (AFM) imaging was modified from Marini et al.[17] Before AFM imaging, the peptide solution was diluted to 5 μM with filtered deionized water adjusted to pH 1, 2, 3, 5, 7, and 9 by adding hydrochloric acid or ammonium hydroxide, and 20 μL of the sample was deposited onto freshly cleaved mica and air-dried for 30 min. The CD profiles showed the characteristic for α-helices with minima at 222 and 208 nm. They show decreased helical content as a function of increased pH value (Supporting Information).

AFM. AFM images were collected using a Nanoscope III (Digital Instruments, Santa Barbara, CA) in tapping mode. The tip used was a force modulation etched silicon probe (Veeco Metrology, Sunnyvale, CA) and had a spring constant of 1−5 N/m, a resonance frequency of 60−100 kHz, a nominal tip radius of curvature 5−10 nm, and a cantilever length of 225 μm. The scanning parameters were usually as follows: RMS amplitude before engaging the tip 1.0−1.2 V, integral gain 0.2−0.8, and proportional gain 0.4−1.6. The set point was usually 0.6−1.0 V and the scanning speed 1.0 Hz. The resolution of the AFM scans was 512 × 512 pixels, which produced topographic images of the peptide on the mica surface. Images were collected on several locations across the mica surface. As a comparison, the peptide at pH 1 and 8.5 was also imaged on a silicon surface. To be certain the fractal patterns were not a contribution from the electrolytes, the solution without peptide was imaged on mica in the same manner. In addition, the peptide was not only imaged with the reducing agent dithiothreitol (DTT) at pH 1 and 5, but also with the hydrophobic solvent acetonitrile, at pH 6.

Dynamic Light Scattering (DLS). DLS was carried out using PDDLS/Batch (Precision Detectors, Franklin, MA). An aliquot of 200 μL at 23 μM was prepared at various pH values. The Precision Deconvolution program was used to calculate the apparent hydrodynamic radius. The intensities of scattered light of different peptide concentrations (1.25, 2.5, 5, 10, 15, and 20 μM) were also analyzed at pH 1. Numbers in legends are averages and standard deviations of the apparent radius of gyration (r_g). Analysis of the DLS intensity at different concentrations (1.25 μM (229,000 counts/second) to 20 μM (539,000 counts/second)) showed that more aggregation took place at higher concentrations, indicating that the large clusters were formed via a mechanism similar to the density-dependent coagulation of colloids.[32] In cases such as our system where the particle size distribution ranges more than an order of magnitude, the light is scattered mostly by the largest clusters, so the DLS reading becomes less sensitive to the smaller clusters.

Molecular Dynamics (MD) Simulations. All molecular dynamics (MD) simulations were performed using CHARMM version 29b1, with the param19 force field. Solvent contribution was accounted for by using the Analytic Continuum Solvent model[36] in CHARMM. The initial coiled-coil was constructed based on the backbone coordinates of the GCN4 (PDB ID: 2ZTA). The structure was initially energy minimized for 1400 steps, and the MD was run by heating from 0 to 300 K for 10 picoseconds, followed by equilibration with the temperature held at 300 K for 90 picoseconds. The final production run was for 500 picoseconds and the time step of the simulation was 2 fs. The coordinates during the production run were averaged and energy minimized to yield the final relaxed structure.

Acknowledgment. We thank Steve Yang for technical assistance with the CD spectrometer and DLS instrument, Hidenori Yokoi for the AFM imaging, and Patrick Kiley for the gel electrophoresis. This work was supported in part by grants from DARPA/AFOSR, MURI/AFOSR, DARPA-

BioComputing, and NSF CCR-0122419 to MIT Media Lab's Center for Bits & Atoms. We also acknowledge the Intel Corporation educational donation of computing cluster to the Center for Biomedical Engineering at MIT. We thank Dr. Benoit Mandelbrot for numerous stimulating discussions.

Supporting Information Available: Verification of the extent of helical structure of the designed coiled-coil as a function of pH changes. This material is available free of charge via the Internet at http://pubs.acs.org.

Note Added in Proof. During the publication process, it came to our attention that a paper relevant to our work has been published. Rapaport and colleagues studied a β-sheet forming peptide at the air/water interface. This peptide, PCFSFKFEP, also contains a cysteine. Upon exposure to air and drying on mica surface, this peptide also formed a fractal structure similar to our observations. (Sneer, R.; Weygand, M. J.; Kjaer, K.; Tirrell, D.; Rapaport, H. *ChemPhysChem* **2004**, *5*, 747−750.)

References

(1) Mandelbrot, B. *The Fractal Geometry of Nature*, 3rd ed.; W. H. Freeman and Company, New York, 1983.
(2) Mandelbrot, B. *Fractals and Chaos. The Mandelbrot Set and Beyond*; Springer-Verlag, New York, 2004.
(3) Masters, B. R. *Annu. Rev. Biomed. Eng*. **2004**, *6*, 427−452.
(4) Lee, J. M.; Yoon, U.; Kim, J. J.; Kim, I. Y.; Lee, D. S.; Kwon, J. S.; Kim, S. I. *IEEE Trans. Biomed. Eng*. **2004**, *51*, 1494−1498.
(5) Majumdar, K. K. *IEEE Trans. Syst. Man. Cybern. B Cybern*. **2004**, *34*, 746−752.
(6) Misawa, M.; Dairoku, I.; Honma, A.; Yamada, Y.; Sato, T.; Maruyama, K.; Mori, K.; Suzuki, S.; Otomo, T. *J Chem Phys*. **2004**, *121*, 4716−4123.
(7) Gratrix, S.; Elgin, J. N., *Phys. Rev. Lett*. **2004**, *92*, 014101.
(8) Halsey, T. C.; Jensen, M. H. *Nature* **2004**, *428*, 127−128.
(9) Butala, H. D.; Sadana, A. *Biosens. Bioelectron*. **2004** *19*, 933−944.
(10) Ahammer, H.; DeVaney, T. T. *Chaos* **2004**, *14*, 183−188.
(11) Whitesides, G. M. *Nat. Biotechnol*. **2003**, *21*, 1161−1165.
(12) Zhang, S. *Nat. Biotechnol.* **2003**, *21*, 1171−1178.
(13) Reches, M.; Gazit, E. *Science* **2003**, *300*, 625−627.
(14) Kroger, N.; Deutzmann, R.; Sumper, M. *J. Biol. Chem*. **2001**, *276*, 26066−26070.
(15) Bratt, L. L.; Stone, M. O. *Nature* **2001**, *413*, 291−293.
(16) Mann, S.; Cölfen, H. *Angew. Chem., Int. Ed*. **2003**, *42*, 2350−2365.
(17) Marini, D.; Hwang, W.; Lauffenburger, D.; Zhang, S.; Kamm, R. *Nano Lett.* **2002**, *2*, 295−299.
(18) Vauthey, S.; Santoso, S.; Gong, H.; Watson, N.; Zhang, S. *Proc. Natl. Acad. Sci. U.S.A.* **2002**, *99*, 5355−5360.
(19) Santoso, S.; Hwang, W.; Hartman, H.; Zhang, S. *Nano Lett.* **2002**, *2*, 687−691.
(20) von Maltzahn, G.; Vauthey, S.; Santoso, S.; Zhang, S. *Langmuir* **2003**, *19*, 4332−4337.
(21) Crick, F. H. *Acta Crystallogr*. **1953**, *6*, 689−697.
(22) Bränden, C.; Tooze, J. *Introduction to Protein Structure*, 2nd ed.; Garland Publishing: New York, 1999.
(23) Beck, C.; Schögl, F. *Thermodynamics of Chaotic Systems*; Cambridge University Press: Cambridge, 1993.
(24) Meakin, P. *Phys. Rev. Lett.* **1983**, *51*, 1119−1122.
(25) Meakin, P. *Phys. Rev. A* **1983**, *27*, 1495−1507.
(26) Skoog, D.; Leary, J. *Principles of Instrumental Analysis*, 4th ed.; Saunders College Publishing: Philadelphia, 1992.
(27) Miura, Y.; Xu, G.-C.; Kimura, S.; Kobayashi, S.; Iwamoto, M.; Imanishi, Y.; Umemura, J. *Thin Solid Films* **2001**, *393*, 59−65.
(28) DeGrado, W. F.; Wasserman, Z. R.; Lear, J. D. *Science* **1989**, *243(4891)*, 622−628.
(29) Witten, T.; Sander, L. *Phys. Rev. Lett.* **1981**, *47*, 1400−1402.
(30) Witten, T.; Sander, L. *Phys. Rev. B* **1983**, *27*, 5686−5697.
(31) Gupta, P.; Rizwan, H., Khan, H.; Saleemuddin, M. *Int. J. Biol. Macromol.* **2003**, *33*, 167−174.
(32) Horng, J.; Demarest, S.; Rsleigh, D. *Proteins: Struct., Funct., Genet.* **2003**, *52*, 193−202.
(33) Zhou, M.; Bentley, D.; Ghosh, I. *J. Am. Chem. Soc.* **2004**, *126*, 734−735.
(34) Ryadnov, M.; Ceyhan, B.; Niemeyer, C.; Woolfson, D. *J. Am. Chem. Soc*. **2003**, *125*, 9388−9394.
(35) Hamad-Schifferli, K.; Schwartz, J.; Santos, A.; Zhang, S.; Jacobsen, J *Nature* **2002**, *415*, 152−155.
(36) Schaefer, M.; Bartels, C.; LeClerc, F.; Karplus, M. *J. Comput. Chem.* **2001**, *22*, 1857−1879.

NL050203R